Available online at www.sciencedirect.com
SCIENCE DIRECT
Cement and Concrete Research 36 (2006) 979–989
Cement and Concrete Research

Predicting carbonation in early-aged cracked concrete

Ha-Won Song [a,*], Seung-Jun Kwon [a], Keun-Joo Byun [a], Chan-Kyu Park [b]

[a] School of Civil and Environmental Engineering, Yonsei University, Seoul 120-479, Republic of Korea
[b] Samsung Corporation Co., LTD, Republic of Korea

Received 2 April 2005; accepted 22 December 2005

Abstract

Carbonation in cracked concrete is considered as one of major deteriorations accelerating steel corrosion in reinforced concrete structures. For durable concrete structures, it is necessary to control crack in concrete through crack resistance evaluation for early-aged concrete structures, but often unavoidable cracks in early-aged concrete may occur. These cracks become a main path for CO_2 penetration inside concrete so that the carbonation is accelerated in cracked concrete.

In this study, an analytical technique for carbonation prediction in early-aged cracked concrete was developed for considering both CO_2 diffusion of pore water in sound concrete and in cracked concrete. Then, characteristics of diffusivity on the carbonation in early-aged concrete are studied through finite element analysis implemented with the so-called multi-component hydration heat model and micro-pore structure formation model. The carbonation behaviour in sound concrete and cracked concrete are also simulated by using the derived diffusivity with consideration of reaction with dissolved CO_2. Finally, numerical results obtained for cracked concrete made with 3 different W/C ratios (45%, 55%, and 65%) with different crack widths were compared with experimental results.
© 2005 Elsevier Ltd. All rights reserved.

Keywords: Concrete; Micro-models; FEM; Carbonation; Early-aged cracks

1. Introduction

The majority of concrete deterioration is connected to corrosion of reinforcement due to carbonation or chloride-induced depassivation of steel bars [1]. In urban and industrial areas, where environmental pollution results in a significant concentration of carbon dioxide, carbonation-initiated reinforcement corrosion prevails. In the case of carbonation, chemical reaction between carbon dioxide from the air and the hydration products of cement in concrete causes a reduction in the alkalinity of concrete and consequently in its ability to protect the steel reinforcement from corrosion [2–6]. To prevent premature deterioration of concrete structures, design and maintenance guidelines have been issued by a number of organizations including the American Concrete Institute [7] and the Canadian Standards Association [8]. Therefore, research is currently conducted at various institutions to develop new and improved construction materials, rehabilitation and repair technologies, and a better understanding of the physical and chemical mechanisms that lead to deterioration. The improved knowledge will enable designers not only to properly rehabilitate and maintain the current stock of concrete structures, but also to improve the durability of future structures by giving, in the design stage, proper consideration to the environment and conditions. Experimental studies on carbonation were conducted by various researchers [9–11]. It was combined with a one-dimensional diffusion model for heat, moisture and CO_2 flow by Saetta et al. [12] who subsequently proposed a two-dimensional extension [13]. The identification of carbonation is an important factor for durability of reinforced concrete structures.

Cracks may easily occur in concrete surface due to heat of hydration, drying shrinkage and improper curing of concrete. During the hydration process of early-aged concrete, external harmful agents like chlorides and CO_2 penetrates through the cracks and it may cause the deterioration of reinforced concrete

* Corresponding author. Tel.: +82 2 2123 2806.
E-mail address: song@yonsei.ac.kr (H.-W. Song).

0008-8846/$ - see front matter © 2005 Elsevier Ltd. All rights reserved.
doi:10.1016/j.cemconres.2005.12.019

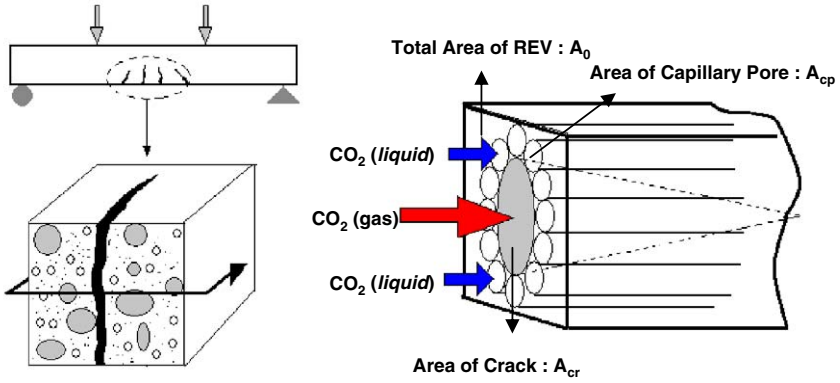

Fig. 1. REV in cracked concrete.

(RC) structures. The early-aged behaviour of concrete has to be evaluated by considering the characteristics of early-aged concrete like hydration, moisture transfer, and micro-pore structure formation which are influenced by concrete mix proportion, curing, and exposure condition for the evaluation of crack resistance in concrete structures [14,15]. Even reaction with dissolved CO_2 and hydrates ($Ca(OH)_2$ and CSH) are recently considered in modeling and analysis of carbonation [16–21], the cracks are not considered or being considered in a least manner. It has reported that, long term cracking has been found to affect the diffusivity of concrete [22]. Studies revealed that, $CaCO_3$ formed during carbonation exceeds that of the hydrates causing decrease in porosity [23,24].

In this study, the carbonation process in cracked concrete is simulated by considering the reaction with dissolved CO_2, $Ca(OH)_2$, and $CaCO_3$ based on the characteristics of early-aged concrete obtained by the so-called multi-component hydration model and micro-pore structure formation model [15,19,25,26]. In order to obtain carbonation behaviour in cracked concrete, an equivalent diffusivity of CO_2 in cracked concrete is derived and their results for carbonation prediction using FEM analysis are verified with experimental results for concrete manufactured with different water–cement ratio (45%, 55% and 65%) and crack widths.

2. CO_2 diffusion in cracked concrete

2.1. Entire flux for CO_2 in sound and cracked concrete

The CO_2 diffusion in cracked concrete can be formulated by averaging the CO_2 diffusion in sound concrete volume, which dose not have cracks, and the CO_2 diffusion in cracked concrete volume having different crack widths. In this paper, an equivalent diffusivity of CO_2 in cracked concrete is derived analytically with an assumption that liquid and gaseous flow rate of CO_2 (mol/s) are constant in the so-called representative element volume (REV) of cracked concrete. A detailed discussion on modeling for early-aged concrete like multi-component hydration model and micro-pore structure formation model and schematics of their interactions can be found in Refs. [15,25,26].

Ishida and Maekawa [19] have provided CO_2 flux and diffusivity as shown in Eqs. (1) and (2), respectively, which utilizes both liquid CO_2 diffusion in saturated pore volume and gaseous CO_2 diffusion in non-saturated pore volume

$$J_{CO_2} = -\left(\frac{\phi D_0^{d}}{\Omega}\int_0^{r_c} dV \frac{\partial \rho_d}{\partial x} + \frac{\phi D_0^{g}}{\Omega}\int_{r_c}^{\infty} \frac{dV}{1+N_K}\frac{\partial \rho_g}{\partial x}\right) \quad (1)$$

$$D_{CO_2} = \frac{\phi(1-S)^4 K_{CO_2}}{\Omega(1+N_K)} D_0^{g} + \frac{\phi S^4}{\Omega} D_0^{d} \quad (2)$$

where J_{CO_2} is entire flux of CO_2, V is pore volume, Ω is average torturity of single pore ($\pi^2/4$), D_0^{d} (1.0×10^{-9} m^2/s) and D_0^{g} (1.34×10^{-9} m^2/s) are basic CO_2 diffusivities for dissolved and gaseous state, respectively, ρ_d and ρ_g (kg/m^3) are concentration of CO_2 for dissolved and gaseous state, respectively, ϕ is porosity, N_K is Knudsen number, S is saturation, K_{CO_2} is equilibrium factor from Henry's Law.

In order to derive the equivalent diffusivity of CO_2 in cracked concrete, an REV is considered as shown in Fig. 1. It is assumed that diffusion paths are composed of only capillary pores and cracks. It is also assumed that each capillary pore can be modeled as each pipe which has constant radii r_i and areas A_i and each crack is modeled as a cone with different diameter varying from maximum crack width r_{cr} to zero.

Total ion flow rate Q_i^{L} (mol/s) in the REV, is equal to the sum of ion flow rate in capillary pores Q_{icp}^{L} (mol/s) and ion flow rate in cracks width Q_{cr}^{L} (mol/s), which is given in Eq. (3).

$$Q_i^{L} = Q_{icp}^{L} + Q_{icr}^{G} = Q_{icp}^{L} + Q_{icr}^{L}\cdot f(\phi S)\cdot K_{CO_2} \quad (3)$$

where $f(\phi S)$ is a resistant function representing the characteristics of paths of the cracks. Local equilibrium condition between liquid state and gaseous state is satisfied in the pore volume but not in the crack width, so that the function $f(\phi S)$ written as Eq. (4) is considered for decrease in carbonation process in cracked concrete with lower W/C ratio.

$$f(\phi S) = 0.002[\phi S]^{-9.1952} \quad (4)$$

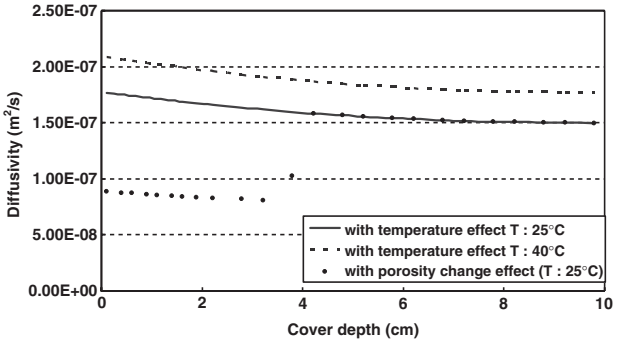

Fig. 2. Diffusivity of CO_2 vs. effect of porosity at various temperatures.

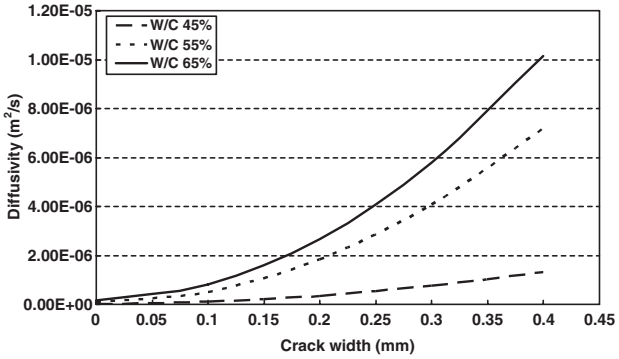

Fig. 3. Diffusivity of CO_2 vs. crack width.

where ϕS is defined as Eq. (5).

$$\phi S = V_0^{\mathrm{L}}/V_0 \tag{5}$$

where V_0^{L} is saturated volume of REV and V_0 is volume of REV. Along with the Fick's 1st Law, ion flow rate $Q_{\mathrm{icp}}^{\mathrm{L}}$ and $Q_{\mathrm{cr}}^{\mathrm{L}}$ can be expressed in Eqs. (6) and (7).

$$Q_{\mathrm{icp}}^{\mathrm{L}} = J_{\mathrm{cp}}^{\mathrm{L}} \sum A_{\mathrm{i}} = -D_{\mathrm{CO_2}} F^{\mathrm{L}} A_{\mathrm{cp}} \tag{6}$$

$$Q_{\mathrm{icr}}^{\mathrm{L}} = J_{\mathrm{cr}}^{\mathrm{L}} \sum A_{\mathrm{i}} = -D_{\mathrm{crack}} F^{\mathrm{L}} A_{\mathrm{cr}} \tag{7}$$

where $J_{\mathrm{cp}}^{\mathrm{L}}$ and $J_{\mathrm{cr}}^{\mathrm{L}}$ are average flux in capillary pore and crack, respectively, and F^{L} (mol/m^4) is concentration gradient in pore solution.

In order to obtain equivalent diffusivity $D_{\mathrm{CO_2}}^{\mathrm{eq}}$ in REV, total saturated area A_0^{L} ($=A_{\mathrm{cp}}+A_{\mathrm{cr}}$) of dissolved CO_2 in total area in the REV is considered as Eq. (8) then, the equivalent diffusivity $D_{\mathrm{CO_2}}{}^{\mathrm{eq}}$ can be obtained from the diffusivity in sound concrete $D_{\mathrm{CO_2}}$ and diffusivity in cracked concrete D_{crack} as Eq. (9).

$$Q_{\mathrm{i}}^{\mathrm{L}} = J_{\mathrm{i}}^{\mathrm{L}} \sum (A_{\mathrm{cp}} + A_{\mathrm{cr}}) = -D_{\mathrm{CO_2}}^{\mathrm{eq}} F^{\mathrm{L}} A_0^{\mathrm{L}} \tag{8}$$

$$D_{\mathrm{CO_2}}^{\mathrm{eq}} A_0^{\mathrm{L}} = D_{\mathrm{CO_2}} A_{\mathrm{cp}} + D_{\mathrm{crack}} A_{\mathrm{cr}} K_{\mathrm{CO_2}} f(\phi S) \tag{9}$$

Eq. (9) can be rewritten as Eq. (10).

$$D_{\mathrm{CO_2}}^{\mathrm{eq}} = \frac{D_{\mathrm{CO_2}}(A_0^{\mathrm{L}} - A_{\mathrm{cr}})/A_{\mathrm{cr}} + D_{\mathrm{crack}} K_{\mathrm{CO_2}} f(\phi S)}{A_0^{\mathrm{L}}/A_{\mathrm{cr}}} \tag{10}$$

Since the ratio of saturated area A_0^{L} to total area A_0 in REV is given as Eq. (11) with average torturity Ω ($=(\pi/2)^2$) of single pore, Eq. (10) becomes Eq. (12).

$$A_0^{\mathrm{L}}/A_0 = \phi S/\Omega \tag{11}$$

$$D_{\mathrm{CO_2}}^{\mathrm{eq}} = D_{\mathrm{CO_2}} + \frac{D_{\mathrm{crack}} K_{\mathrm{CO_2}} f(\phi S)\Omega}{R_{\mathrm{a}} \phi S} \tag{12}$$

where R_{a} is defined as the ratio of total area A_0 to crack area A_{cr} which is equivalent to the area of the cone ($\pi r_{\mathrm{cr}}^2/3$) in the REV as Eq. (13).

$$R_{\mathrm{a}} = A_0/A_{\mathrm{cr}} \tag{13}$$

In the REV, since CO_2 diffusion in crack is almost same as CO_2 diffusion D_0^{g} in the air, the $D_{\mathrm{CO_2}}{}^{\mathrm{eq}}$ in REV of Eq. (2) can be rewritten as Eq. (14).

$$D_{\mathrm{CO_2}}^{\mathrm{eq}} = \frac{\phi(1-S)^4 K_{\mathrm{CO_2}}}{\Omega(1+N_{\mathrm{K}})} D_0^{\mathrm{g}} + \frac{\phi S^4}{\Omega} D_0^{\mathrm{d}} + \frac{D_0^{\mathrm{g}} K_{\mathrm{CO_2}} f(\phi S)\Omega}{R_{\mathrm{a}} \phi S} \tag{14}$$

Eq. (14) shows that increased crack width r_{cr} considered in R_{a} accelerates diffusion of CO_2 in cracked concrete.

2.2. Temperature effect on CO_2 diffusion

As temperature goes up, the solubility of CO_2 is decreased and acid formation is also decreased, but diffusivity of CO_2 is increased due to increased activity energy. The temperature dependence on diffusion follows Arrhenius's Law. It is shown that activity energy of CO_2 is almost constant in certain temperature range (20~40 °C) regardless of W/C ratios of concrete [27]. Basically, the temperature effect should be considered in carbonation reaction because the solubility-product constant and Henry's constant of CO_2 are dependent on temperature. But we consider the temperature effect on diffusivity only to Arrhenius's Law for the sake of simplicity in analysis. The temperature effect on diffusivity of CO_2 is given in Eq. (15).

$$D(T) = D_{\mathrm{ref}} \cdot \exp\left[\frac{U}{R}\left(\frac{1}{T_{\mathrm{ref}}} - \frac{1}{T}\right)\right] \tag{15}$$

where D_{ref} is reference diffusivity (same as $D_{\mathrm{CO_2}}^{\mathrm{eq}}$ in cracked concrete and $D_{\mathrm{CO_2}}$ in sound concrete), U (8500 Cal/mol K) is

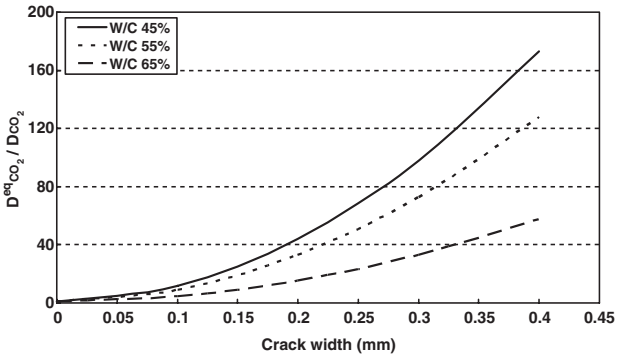

Fig. 4. Ratio of $D_{\mathrm{CO_2}}^{\mathrm{eq}}/D_{\mathrm{CO_2}}$ vs. crack width for various W/C ratios.

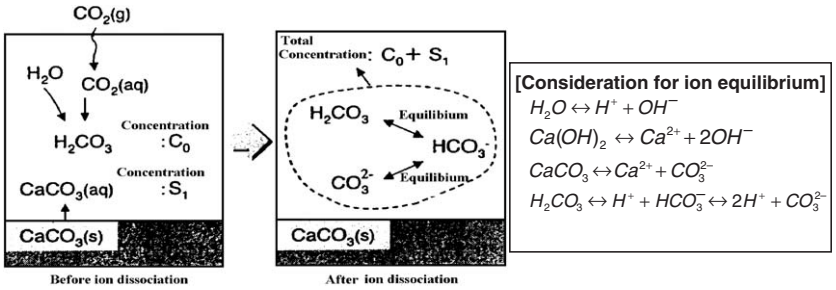

Fig. 5. Mass balance and equilibrium conditions for carbonic acid [19].

activity energy of CO_2, and T_{ref} (298 K) is reference temperature.

2.3. Porosity change effect on CO_2 diffusion

In general, the diffusivity coefficient of CO_2 is obtained by experiments with N_2 or O_2 multiplied by the molecular mass ratio of CO_2, so that if CO_2 gas is used, the diffusivity coefficient is changed by porosity change due to carbonation process. It is well known that dissolved CO_2 reacts with hydrates and forms $CaCO_3$ and the volume of hydrates is increased due to carbonation process [16–18]. It is also reported that the reduction in pore volume observed for the cement matrices could be associated with the deposition of $CaCO_3$ formed during carbonation. The volume of the $CaCO_3$ formed exceeds that of the hydrates, thus causing a reduction in porosity [23]. Change in porosity is reported to be more decreased in concrete with relatively lower W/C ratio [24].

The diffusion coefficient of CO_2 in concrete cannot be measured experimentally, because carbonation takes place already during testing and falsifies the measurements. Therefore oxygen is used as an inert gas to determine the diffusion coefficient [28]. As per study [29], which showed 50% of decrease in porosity before carbonation, is considered for this study as Eq. (16).

$$\begin{aligned} \phi(R) &= \phi\cdot(-1.25R+1) \quad 0.0\le R\le 0.4 \\ \phi(R) &= 0.5\phi \quad 0.4< R\le 1.0 \end{aligned} \tag{16}$$

where $\phi(R)$ is the porosity function for carbonation process, ϕ is porosity before carbonation, and R is the ratio of the amount of $Ca(OH)_2$ consumed to total amount of $Ca(OH)_2$(=consumed weight of $Ca(OH)_2$ / weight of $Ca(OH)_2$ before carbonation). If the effect of temperature and the effect of porosity change are applied to both sound concrete and cracked concrete, then the equivalent diffusivity can be rewritten as Eq. (17).

$$\begin{aligned} D_{CO_2}^{eq} = &\left[\frac{\phi(R)(1-S)^4 K_{CO_2}}{\Omega(1+N_K)} D_0^g + \frac{\phi(R)S^4}{\Omega} D_0^d \right. \\ &\left. + \frac{D_0^g K_{CO_2}\Omega[0.002(\phi(R)S)]^{-9.1952}}{R_a\phi(R)S}\right] \\ &\cdot \exp\left[\frac{U}{R}\left(\frac{1}{T_{ref}}-\frac{1}{T}\right)\right] \end{aligned} \tag{17}$$

Fig. 2 shows the simulated diffusivity coefficient by the effect of temperature and porosity change during carbonation process. The exposure condition is 10% concentration of CO_2 and 65% relative humidity, W/C:65% and calculated carbonation depth is 4 cm. The increased diffusivity coefficient due to change in temperature (20 and 40 °C) and decreased diffusivity coefficient in carbonation area can be found in the Fig. 2. The effect of crack width on equivalent diffusivity is shown in Fig. 3. Fig. 4 shows the behaviour of $D_{CO_2}^{eq}/D_{CO_2}$ vs. crack width for different W/C ratios.

From Fig. 2 it is observed that, as the temperature increases the diffusivity also increased due to increased activation energy. The temperature effect is very pronounced in carbonation, because the diffusivity of CO_2 is dependent on temperature. It is also found that as the cover depth increases the diffusivity is also found to decreases.

From Fig. 3 it is observed that, as the water cement ratio increases the CO_2 diffusivity is also found to be increased irrespective of the crack width. As the crack width increased from 0.05 to 0.45 mm, the CO_2 diffusivity also increases with

Table 1
The terms used in governing equation for mass and energy conservation

Variables [X_i]	Potential term	Flux term	Sink term
T [temperature]	ρC[Kcal/K.m^3]: Constant	$-K_H\nabla T$ [Kcal/m^2 s]: Constant	Q_H[Kcal/m^3 s]: Multi component hydration model of cement
P [pore pressure]	$\phi\rho\frac{\partial S}{\partial P}$[kg/Pa m^3]: Path dependent moisture isotherms	$-(K_l+K_v)\nabla P$ [kg/ m^2 s]: Random geometry of pores and Knudsen vapour diffusion	$-Q_{hyd}-\frac{\partial(\rho S\phi)}{\partial t}$ [kg/m^3 s]: Water combined due to hydration; bulk porosity change effect
C [CO_2 concentration]	$\phi(1-S)K_{CO_2}+\phi S$ [mol l/mol m^3]: Path dependent transport of mass, Porosity change dependent	$-D_{CO_2}^{eq}\nabla C$ or $-D_{CO_2}\nabla C$ [mol/m^2 s]: Mass and Knudsen diffusion in sound and/or cracked surface, Temperature and porosity change dependent	Q_{CO_2} [mol/m^3 s]: CO_2 consumption due to carbonation process

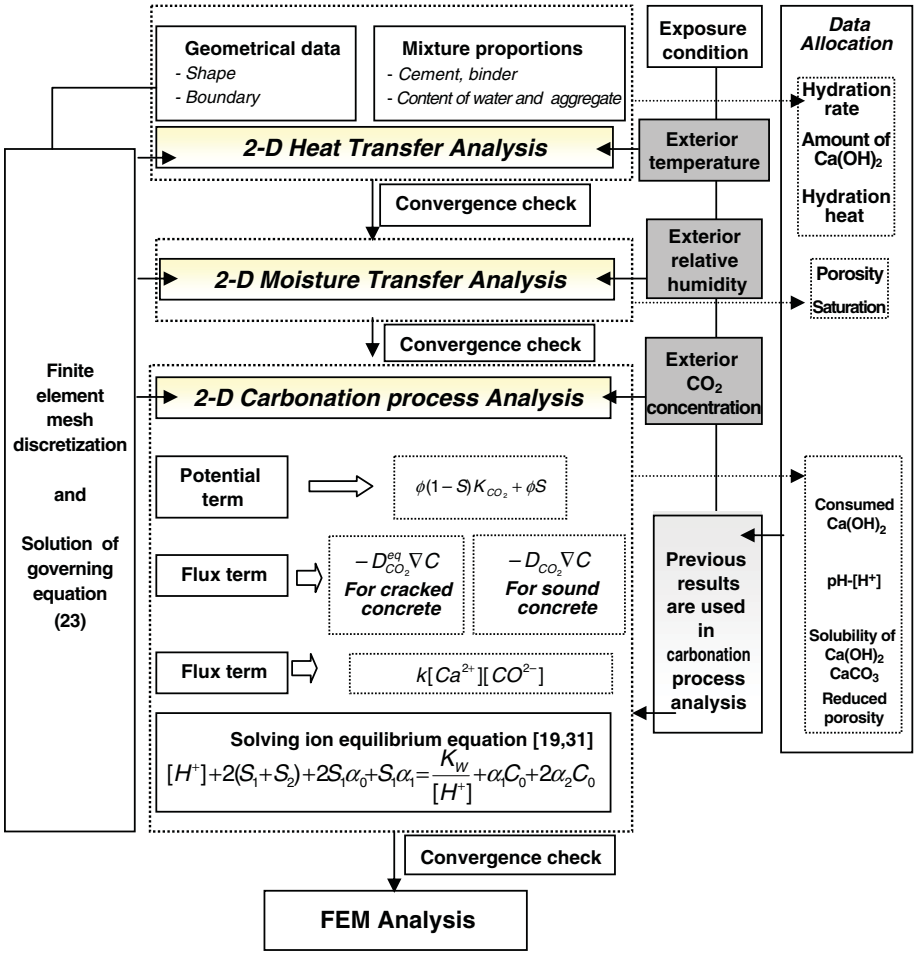

Fig. 6. Computational scheme of coupled modeling of carbonation in cracked concrete.

reference to different W/C ratios. Carbonation has a clear influence on the porosity and this decrease is more important for higher W/C ratios. The porosity decreases as the carbonation proceeds. This is in agreement with the findings of other researchers [30].

From Fig. 4 it is observed that, as the crack width and W/C ratio increases, the diffusion coefficient $D^{eq}_{CO_2}/D_{CO_2}$ also increases proportionately.

Cracks irrespective of their nature, have a considerable influence on the moisture permeability of cementitious materials. As a consequence, the transport of aggressive substances is promoted and the degradation process is further accelerated. It is also reported that long term cracking has been found to affect the diffusivity of concrete [22]. It has also been reported that the diffusivity of the material can be increased by a factor ranging from 2 to 10. The presence of continuous cracks tends to markedly modify the transport coefficient of the solid. Results obtained with the model indicate that the influence of cracking tends to be more significant when the ratio D_1/D_0 is increased. This essentially means the affect of cracking is relatively more important for dense materials. Continuous cracks favour locally the penetration of ions. It may also contribute to accelerate the

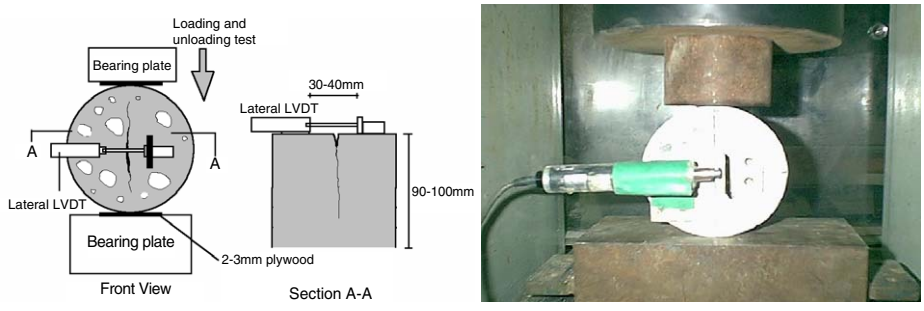

(a) Splitting test setup (b) Photo for splitting test

Fig. 7. Scheme for crack-inducing.

Table 2
Mix proportions of concrete specimens

W/C	Slump (cm)	Water (kg/m^3)	Cement (kg/m^3)	Sand (kg/m^3)	Coarse aggregate (kg/m^3)
45	15	191	424	668	1058
55	15	184	335	762	1058
65	15	182	280	829	1041

local dissolution of solid phases that may subsequently affect the material behaviour.

3. Modeling for CO_2 transport and reaction of carbonation

3.1. Governing equation for CO_2 transport

In this section, the mass balance conditions for carbon dioxide in a porous medium are formulated. Two phases of carbon dioxide existing in concrete are considered; gaseous carbon dioxide and carbon dioxide dissolved in pore water. By solving the mass balance equation under given initial and boundary conditions, the non-steady state condition of carbon dioxide is quantified as Eq. (18).

$$\frac{\partial}{\partial t}[\phi(1-S)\cdot\rho_g + \phi S\cdot\rho_d] + \mathrm{div}J_{CO_2} - Q_{CO_2} = 0 \tag{18}$$

where ϕ is total porosity as transfer route and storage, S is saturation, ρ_g and ρ_d are density of gaseous and dissolved CO_2 density (kg/m^3), respectively. J_{CO_2} is total flux of dissolved and gaseous CO_2 (kg/m^2 s). The first term in Eq. (18) represents the rate of change in total amount of CO_2 per unit time and volume, the second term is the flux of CO_2, and the third term Q_{CO_2} is a sink term. The above equation gives the concentration of gaseous and dissolved CO_2 with time and space. In previous studies [16–18], the formation of hydrate and porosity characteristics are obtained from regression analysis as Power Law, but in this paper, the so-called Multi-Component Hydration Heat Model (MCHHM) and Micro-Pore Structure Formation Model (MPSFM) are utilized for system dynamics for Eq. (18).

3.2. Equilibrium condition for gaseous and dissolved CO_2

The local equilibrium between gaseous and dissolved CO_2 is represented by Henry's Law and Dalton's Law, which state the relationship between gas solubility in pore water and the partial gas pressure as Eq. (19).

$$P_{CO_2} = H'_{CO_2}\cdot\rho'_d, \tag{19}$$

where P_{CO_2} is equilibrium partial pressure of carbon dioxide in the gas pressure (Pa), ρ'_d is mole fraction (CO_2 mol/solution mol), H'_{CO_2} is Henry constant (1.45×10^8 Pa/mol fraction, at 25 °C). For one cubic meter of dilute solution, the moles of water in the solution, n_{H_2O} will be 5.56×10^4 (mol/m^3). Accordingly, the concentration of dissolved CO_2 per cubic meter of solution, ρ_d (kg/m^3) can be expressed as Eq. (20).

$$\rho_d = \frac{P_{CO_2}}{H'_{CO_2}}\cdot n_{H_2O}\cdot M_{CO_2} = \frac{P_{CO_2}}{H_{CO_2}} \tag{20}$$

where M_{CO_2} is molecular mass of CO_2 (0.044 kg/mol). Eq. (19) can be rewritten as Eq. (21) with assumption of perfect-gas equation.

$$P_{CO_2} = \frac{\rho_g RT}{M_{CO_2}} \tag{21}$$

where R is gas constant (J/mol K), T is absolute temperature (K).

After the dissolution, CO_2 reacts with calcium ions, and so the concentration of dissolved CO_2 can fluctuate from the above equilibrium condition. The equilibrium condition cannot be formulated by Henry's Law alone; it is also necessary to determine the amount of dissolved CO_2 based on the rate of chemical reactions, which represents kinetic fluctuations dependent on the distribution of CO_2 concentration. However, it is very difficult to take into account such kinetic fluctuations as it is, and in fact, it is expected that the rate of CO_2 gas dissolution will be faster when the partial pressure of CO_2 gas becomes large. For these reasons, in this model we assume that the amount of dissolved CO_2 can be approximately described by Henry's Law [17,27].

3.3. Modeling of carbonation process

Ishida and Maekawa have proposed the carbonation reaction with solubility of $Ca(OH)_2$, $CaCO_3$ [19,25,26]. The rate of CO_2 consumption due to carbonation can be expressed by the following differential equation as Eq. (22), assuming that the reaction is the first order with respect to $[Ca^{2+}]$ and $[CO_3^{2-}]$ concentration.

$$Ca^{2+} + CO_3^{2-} \rightarrow CaCO_3,\ \frac{\partial(C_{CaCO_3})}{\partial t} = k[Ca^{2+}][CO_3^{2-}] \tag{22}$$

where C_{CaCO_3} (mol/l) is concentration of calcium carbonate and k (2.04 l/mol s) is reaction rate coefficient. Calcium ions

Table 3
Condition of accelerated carbonation test

CO_2 concentration	Temperature	R.H.	Exposure period	Duration of measurement
10%	25±0.5 (°C)	65±5%	3 months	2 weeks

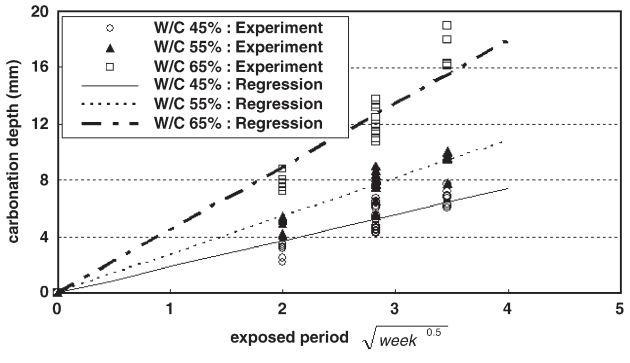

Fig. 8. Carbonation depth in sound concrete.

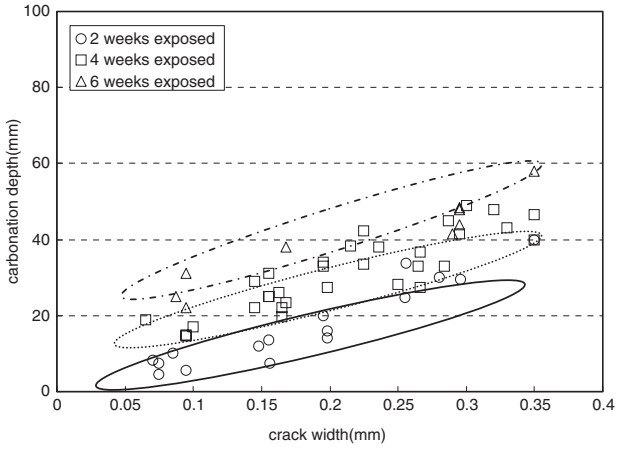

(a) Carbonation depth in cracked concrete (W/C 45%)

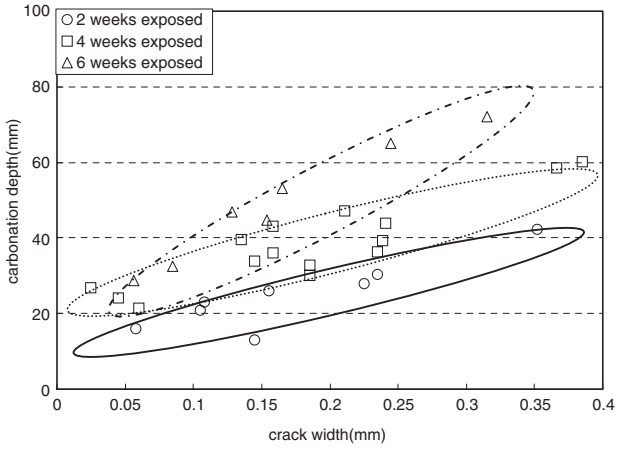

(b) Carbonation depth in cracked concrete (W/C 55%)

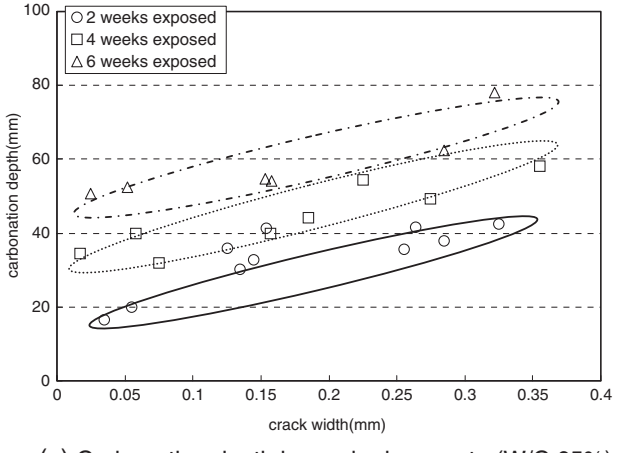

(c) Carbonation depth in cracked concrete (W/C 65%)

Fig. 9. Carbonation depth in cracked concrete.

resulting from the dissolution of $Ca(OH)_2$ are assumed to react with carbonate ions, whereas the reaction of silicic acid calcium hydrate (CSH) is not considered. This is based on the fact that the solubility of CSH is quite low compared with that of $Ca(OH)_2$. In order to calculate the reaction rate, the relation of ion equilibriums and mass balance as shown in Fig. 5 are considered. A detailed discussion of the carbonation reaction and carbonation process can be found in Refs. [19,25,26,31].

4. Modeling of coupled heat transfer, moisture transport and carbonation process in cracked concrete

In order to simulate carbonation process in cracked concrete, hydrates $Ca(OH)_2$, saturation, and porosity in early-aged concrete should be obtained using governing equation for mass and energy conservation in porous media given by Eq. (23)

$$\alpha_i \frac{\partial X_i}{\partial t} + \mathrm{div} J_i (D_i \nabla X_i) - Q_i = 0 \tag{23}$$

where, the first term is potential term, the second term is flux term and the last term is sink term of $[X_i]$ in Eq. (23). The details of $[X_i]$ and composition terms are explained in Table 1.

From Table 1, ρC is specific heat capacity, K_H is heat conductivity, Q_H is heat generation rate, K_l and K_v are liquid and vapour conductivities, Q_{hyd} is combined water due to hydration. In order to apply this dynamic system to cracked concrete, $D^{eq}_{CO_2}$ considering the temperature effect and porosity change rate is considered to flux term in each time and space. A computational scheme of coupled modeling of carbonation in cracked concrete is shown in Fig. 6.

5. Verification of the test results for sound concrete and cracked concrete

5.1. Experimental program

Cylindrical concrete specimens of size 10 cm diameter and 20 cm height with different W/C ratios (45%, 55%, and 65%) were cast for accelerated carbonation test. After 24 h the specimens were demoulded and cured under water for 28 day (20 °C). After curing, the concrete specimens were kept in humidity chamber for 2 weeks at 65% R.H. condition. For 1-D carbonation process, except the top surface other sides of the specimens are coated with wax.

For carbonation in cracked concrete, the cracks are induced into the specimens by splitting test. To measure the

Table 4
Carbonation result in sound and cracked concrete

Condition	$Y = A\sqrt{T}$: (mm/week$^{0.5}$)					
	W/C 45%		W/C 55%		W/C 65%	
Crack width	A	R^2	A	R^2	A	R^2
0 (sound surface)	1.856	0.8459	2.705	0.8459	4.472	0.9057
0.0–0.1 mm	8.984	0.8710	12.158	0.9955	22.283	0.9288
0.1–0.2 mm	13.798	0.9363	18.265	0.9705	22.283	0.9887
0.2–0.3 mm	18.767	0.9901	23.658	0.9548	25.904	0.9982
Over 0.3 mm	24.107	0.9764	29.562	0.9998	30.671	0.9939

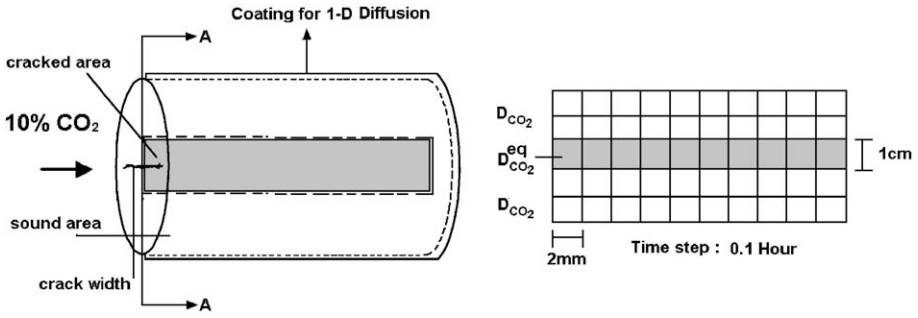

Fig.10. Modelling for carbonation process and FEM.

induced crack width, LVDT is installed on the surface of specimens, perpendicular to direction of crack propagation. The crack width measured in loading step is wider than in unloading step so we measured crack width in fully unloaded state. It is very difficult to obtain required crack width so that we have tried to sort out the crack width by 0.1 mm-division after splitting test. The splitting test setup is shown in Fig. 7. Mix proportions of concrete specimens are shown in Table 2, and procedures of accelerated carbonation test are shown in Table 3.

5.2. Experimental results of carbonation depth in sound and cracked concrete

The fresh-cut surfaces of each slice (sound and cracked) were cleaned and sprayed with a phenolphthalein pH-indicator. The results of carbonation test in sound and cracked concrete are shown in Figs. 8 and 9 (a, b and c), respectively. From Fig. 8 it is observed that the carbonation depth increases with the exposure period. The experimental result in sound concrete are regressed with, so-called, the square root-*t* equation and those

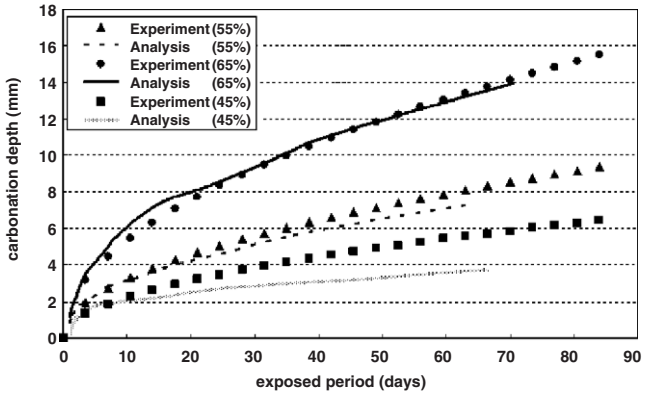

(a) Experimental results in sound concrete

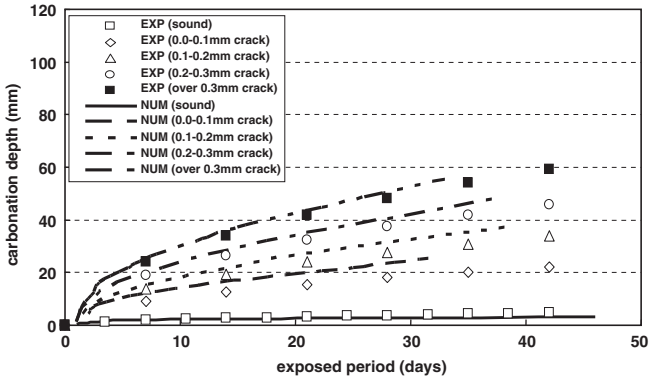

(b) Experimental results in cracked concrete (W/C 45%)

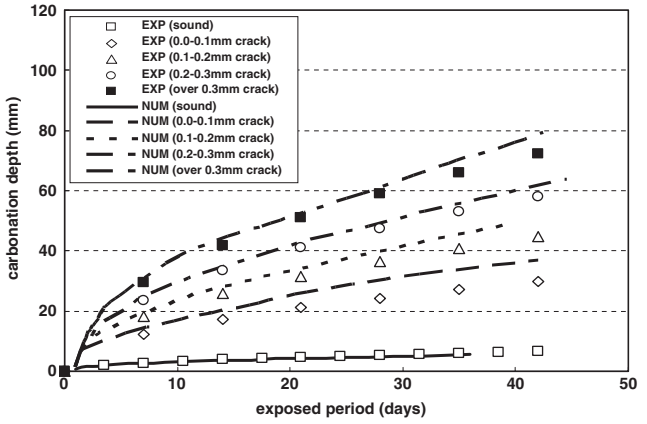

(c) Experimental results in cracked concrete (W/C 55%)

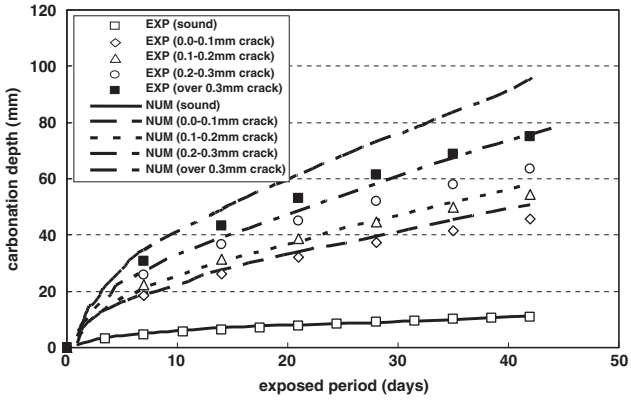

(d) Results in cracked concrete (W/C 65%)

Fig. 11. Effect of cracks and *W*/*C* ratio in carbonation process.

in cracked concrete are plotted with crack widths. The circles in Fig. 9 clearly show that the carbonation process is faster with higher W/C ratios and larger crack width. The detailed results in carbonation test are shown in Table 4. For simplicity and convenience of expression, the crack widths of specimens are sorted out in 0.1 mm-interval.

From Fig. 9 it is observed that, as the crack width increases the carbonation depth also increases with increase in W/C ratio and exposure period. It is a well known fact that, as the crack width increases, atmospheric (gaseous and dissolved) CO_2 enters through the crack and it deteriorate the concrete in terms of carbonation by forming $CaCO_3$ and reducing the alkalinity of the concrete, which reduces the durability of concrete. Table 4 represents the carbonation results in sound and cracked concrete.

5.3. Verification and comparison

Mesh for FEM analysis is shown in Fig. 10 and numerical results are compared with experimental results in Fig. 11. The depth of carbonation on sound and cracked concrete can be predicted well by the proposed scheme. Both experimental and numerical results show the traditional trend of carbonation with time. In the case of low W/C ratio, relatively slow carbonation is measured. With the increase in crack widths and W/C ratios, rapid carbonation is obtained. The effect of cracks on carbonation process is obtained to be more critical for concrete with higher W/C ratio.

5.4. Application examples for long term exposure condition

5.4.1. Parameters for long term effect in the model

Application examples of long term exposure condition are performed through the proposed model. In contrast with accelerated carbonation test, CO_2 concentration is so small (about 0.03~0.065%) that the carbonic reaction constant, λ is considered to be modified for reasonable accuracy [24]. The Eq. (22) for carbonic reaction is modified to Eq. (24).

$$\frac{\partial (C_{CaCO_3})}{\partial t} = k \cdot \lambda \cdot [Ca^{2+}][CO_3^{2-}] \tag{24}$$

where λ is constant (=5~20) for low concentration of CO_2.

Furthermore, the CO_2 diffusivity in cracked concrete is dependent on environmental condition such as local saturation, auto healing (crack-closing) as well as concentration of CO_2.

Table 5
Mixture proportion and environmental condition

W/C(%)	C (kg/m^3)	G (kg/m^3)	S (kg/m^3)	Slump (cm)
55	335	1058	762	15
Underground	Exterior temperature : 18 °C		CO_2 concentration : 670 ppm	
	Relative humidity : 65.3%		Exposed period : 20.0 years	
Aboveground	Exterior temperature : 18 °C		CO_2 concentration : 340 ppm	
	Relative humidity : 80.0%		Exposed period : 18.3 years	

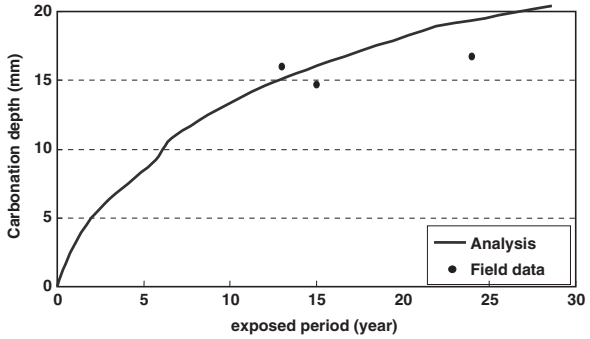

Fig. 12. Comparison of numerical data with field data (underground structure of sound concrete).

But it is very difficult to perform quantitative modeling for the phenomena so equivalent diffusivity of CO_2 can be modified for reasonable accuracy as Eq. (25) for the sake of simplicity.

$$D_{CO_2}^{eq} = \left[\frac{\phi(R)(1-S)^4 K_{CO_2}}{\Omega(1+N_K)} D_0^g + \frac{\phi(R)S^4}{\Omega} D_0^d + \frac{D_0^g K_{CO_2} \Omega [0.002(\phi(R)S)]^{-9.1952}}{R_a \phi(R) S} \cdot \kappa \right] \cdot \exp\left[\frac{U}{R} \left(\frac{1}{T_{ref}} - \frac{1}{T} \right) \right] \tag{25}$$

where κ is crack parameter considering long term exposure condition as Eq. (26).

$$\kappa = 0.1 \cdot C_{CO_2} \tag{26}$$

where is C_{CO_2} partial volume pressure of CO_2, i.e., concentration of CO_2 (%).

5.4.2. Carbonation in sound and cracked concrete under long term exposure condition

For verification of the proposed model, field data of an underground structure is selected. For the analysis of field data the following mix proportions and environmental conditions are adopted as shown in Table 5.

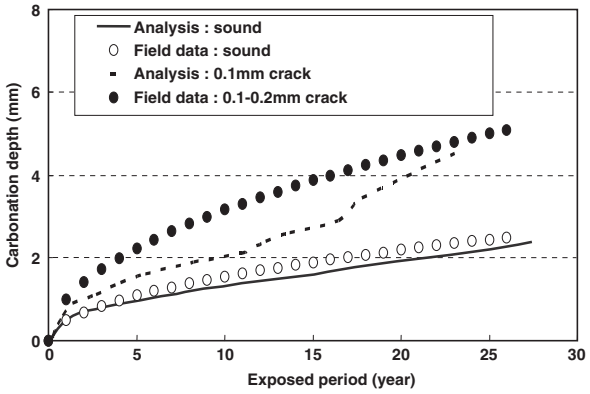

Fig. 13. Comparison of numerical results with field data (aboveground structure of sound/cracked concrete).

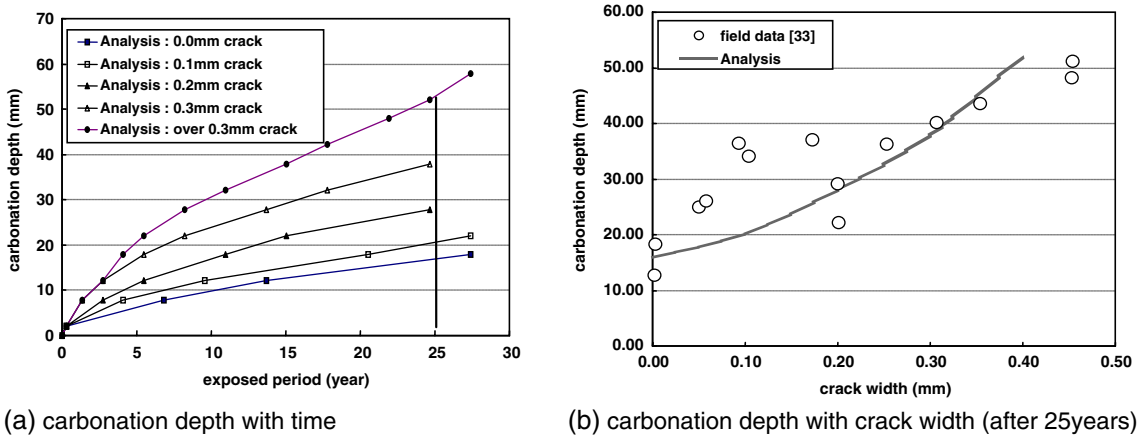

(a) carbonation depth with time

(b) carbonation depth with crack width (after 25years)

Fig. 14. Numerical results with field data in cracked concrete.

The numerical result with field data is shown in Fig. 12 and the proposed model can predict the carbonation depth with reasonable accuracy. Fig. 13 shows the numerical results with field data of carbonation depth for RC column located in outdoor condition (aboveground). The field data shows slow carbonation depth because of low humidity due to variation of environmental condition such as rain or drainage water. The exposed period of the structures is 18.3 years and exterior concentration of CO_2 is assumed to be 340 ppm for normal condition. The slow carbonation velocity in outdoor condition is also reported by previous studies [6,32].

For comparison of numerical data with field data of cracked concrete, previous work [33] is referred but it is assumed that for carbonated concrete the compressive strength was 20~24 Mpa and exposure period is 20~25 years. The numerical results for carbonation in cracked concrete is shown in Fig. 14 with field data.

As shown in Fig. 14, the numerical analysis can well predict the carbonation depth except that the carbonation depths from numerical analysis for the case of small crack width (0.0~0.1 mm) are slightly over estimated those from field data. This difference is thought to be based on the fact that the increased flux term with crack in proposed technique is assumed to be in proportion to squared crack width.

6. Conclusions

The following conclusions were drawn from the above investigation:

- The carbonation prediction technique along with multi component hydration model and micro-pore structure formation model is capable of handling diffusivity of CO_2, by considering the material behaviours like porosity, saturation, and temperature effects as well as porosity change during carbonation process in early-aged concrete.
- Comparison of experimental data with numerical results obtained shows that the proposed model can predict the carbonation depth in cracked concrete with reasonable accuracy.
- The developed model can be used as a tool to evaluate the durability rating of reinforced concrete structures and thus may help avoiding damage due to carbonation.

Acknowledgment

The authors wishes to acknowledge Prof. Koichi Maekawa of the Univ. of Tokyo for the valuable advice and SAMSUNG Corporation Co., LTD. for financial support.

References

[1] P.A.M. Basheer, S.E. Chidiac, A.E. Long, Predictive models for deterioration of concrete structures, Constr. Build. Mater. 10 (1996) 27–37.
[2] G.J. Verbeck, Mechanisms of corrosion in concrete, Corrosion of Metals in Concrete, SP-49, ACI, 1975, pp. 21–38.
[3] L.J. Parrott, Carbonation, moisture, and empty pores, Adv. Cem. Res. 4 (15) (1991) 111–118.
[4] R.J. Currie, Carbonation Depths in Structural Quality Concrete, Building Research Establishment Report Watford, UK, 1986, 19 pp.
[5] D.W.S. Ho, R.K. Lewis, Carbonation of concrete and its prediction, Cem. Concr. Res. 17 (1987) 489–504.
[6] H.J. Wierig, Long time studies on the carbonation of concrete under normal outdoor exposure, RILEM Symposium on Durability of Concrete under Normal Outdoor Exposure, Hanover, Germany, 1984, pp. 192–196.
[7] ACI Committee 201, Guide to Durable Concrete (ACI 201.2R-92).
[8] CAN/CSA-A23.1/A23.2-00, Concrete Materials and Methods of Concrete Construction/Methods of Test for Concrete, 2000.
[9] L. Jiang, B. Lin, Y. Cai, A model for predicting carbonation of high-volume fly ash concrete, Cem. Concr. Res. 30 (2000) 699–702.
[10] W.P.S. Dias, Reduction of concrete sorptivity with age through carbonation, Cem. Concr. Res. 30 (2000) 1255–1261.
[11] S.K. Roy, K.B. Poh, D.O. Northwood, Durability of concrete-accelerated carbonation and weathering studies, Build. Environ. 34 (1999) 597–606.
[12] A.V. Saetta, B.A. Schrefler, R. Vitaliani, The carbonation of concrete and the mechanism of moisture, heat and carbon dioxide flow through porous materials, Cem. Concr. Res. 23 (1993) 761–772.
[13] A.V. Saetta, B.A. Schrefler, R. Vitaliani, 2-D model for carbonation and moisture/heat flow in porous materials, Cem. Concr. Res. 25 (1995) 1703–1712.
[14] H.-W. Song, H.-J. Cho, S.-S. Park, K.-J. Byun, K. Maekawa, Early-age cracking resistance evaluation of concrete structure, Concr. Sci. Eng. 3 (2001) 62–72.

[15] K. Maekawa, R. Chaube, T. Kishi, Modelling of Concrete Performance, E&FN SPON, 1999.
[16] V.G. Papadakis, C.G. Vayenas, M.N. Fardis, Reaction engineering approach to the problem of concrete carbonation, J. AICHE 35 (1989) 1639–1650.
[17] V.G. Papadakis, C.G. Vayenas, M.N. Fardis, Fundamental modeling and experimental investigation of concrete carbonation, ACI Mater. J. 88 (1991) 363–373.
[18] V.G. Papadakis, C.G. Vayenas, M.N. Fardis, Physical and chemical characteristics affecting the durability of concrete, ACI Mater. J. 8 (1991) 186–196.
[19] T. Ishida, K. Maekawa, Modeling of ph profile in pore water based on mass transport and chemical equilibrium theory, Concrete Library of JSCE 37 (2001 June) 151–166.
[20] A. Castel, R. Francois, G. Arliguie, Effect of loading on carbonation penetration in reinforced concrete element, Cem. Concr. Res. 29 (1999) 561–565.
[21] O.B. Isgor, A.G. Razaqpur, Finite element modeling of coupled heat transfer, moisture transfer and carbonation processes in concrete structures, Cem. Concr. Compos. 26 (2004) 57–73.
[22] B. Gerard, J. Marchand, Influence of cracking on the diffusion properties of cement-based materials: Part I. Influence of continuous cracks on the steady state regime, Cem. Concr. Res. 30 (1) (2000) 37–43.
[23] V.T. Ngala, C.L. Page, Effects of carbonation on pore structure and diffusional properties of hydrated cement paste, Cem. Concr. Res. 27 (7) (1997) 995–1007.
[24] T. Ishida, M. Soltani, K. Maekawa, Influential parameters on the theoretical prediction of concrete carbonation process, Proc. 4th International Conference on Concrete Under Severe Conditions, Seoul, Korea, 2004, pp. 205–212.
[25] T. Ishida, K. Maekawa, Modeling of durability performance of cementitious materials and structures based on thermo–hygro physics, Rilem Proceedings Pro 29, Life Prediction and Aging Management of Concrete Structures, 2003, pp. 39–49.
[26] K. Maekawa, T. Ishida, T. Kishi, Multi-scale modeling of concrete performance-integrated material and structural mechanics, Adv. Concr. Technol. 1 (2003) 91–119.
[27] T. Saeki, H. Ohga, S. Nagataki, Mechanism of carbonation and prediction of carbonation process of concrete, Concrete library of JSCE 17 (1991 June) 23–36.
[28] T. Saeki, H. Ohga, S. Nagataki, Change in micro-structure of concrete due to carbonation, Concrete library of JSCE 18 (1991 Dec.) 1–11.
[29] A. Steffens, D. Dinkler, H. Ahrens, Modelling carbonation for corrosion risk prediction of concrete structures, Cem. Concr. Res. 32 (6) (2002) 935–941.
[30] T. Van Gervan, D. Van Baelen, V. Dutree, Vandecasteele, Influence of carbonation and carbonation methods on leading of metals from mortars, Cem. Concr. Res. 34 (1) (2004) 149–156.
[31] H. Freise, Q. Fernando, Ionic Equilibrium in Analytical Chemistry, John Wiley & Sons, Inc., 1963.
[32] I. Izumi, D. Kita, H. Maeda, Carbonation, Kibodang Publication, 1986 in Japanease.
[33] Y. Abe, Result of reference review on crack width effect to carbonation of concrete, Proc. of Symposium on Rehabilitation of Concrete Structures, 1999 Jan., pp. 7–14.